Optical studies of the charge-density-wave phase transition in $Lu_5Rh_4Si_{10}$

H. L. Liu, G. S. Wu, and J. L. Her
Department of Physics, National Taiwan Normal University, Taipei 116, Taiwan

H. D. Yang
Department of Physics, National Sun-Yat-Sen University, Kaohsiung 804, Taiwan

(Received 27 July 2005; revised manuscript received 7 September 2005; published 2 November 2005)

The optical reflectance of the ternary rare-earth intermetallic material $Lu_5Rh_4Si_{10}$ has been measured over a wide frequency range (50–55 000 cm^{-1}) and at temperatures between 15 and 300 K. The charge-density-wave (CDW) transition ($T_{CDW} \sim 147$ K) in this compound manifests itself as a progressive transfer of the Drude spectral weight into the midinfrared absorption bands, leading to the formation of a pseudogap with $2\Delta \sim 5.9k_BT_{CDW}$. Moreover, calculations of the effective number of electrons from the optical conductivity and the fits to the reflectance indicate that approximately 4% of the Fermi surface is destroyed at T_{CDW}. The rest retains its three-dimensional metallic characters. All of these observables support the suggestion of a strongly coupled CDW transition in $Lu_5Rh_4Si_{10}$.

DOI: 10.1103/PhysRevB.72.205102 PACS number(s): 71.45.Lr, 74.25.Gz

I. INTRODUCTION

Since they were first synthesized in the 1980s,[1–3] the subject of superconductivity and other competing broken-symmetry ground states in the ternary rare-earth transition-metal silicides $R_5T_4Si_{10}$ (R=rare-earth ions; T=Co, Ir, Rh, and Os) has been of continued interest to experimentalists and theorists alike.[4–13] In this class of materials, the highest superconducting transition temperature (T_c) to date is 9.1 K in $Y_5Os_4Si_{10}$.[14] More recently, an interesting aspect of these systems is the observation of the multiple charge-density-wave (CDW) instabilities occurring at temperature above T_c.[15,16] This particular feature of the ternary silicides is especially intriguing in view of a delicate balance of competing interactions producing density-wave and superconducting pairing.

Among a number of the ternary silicides with various combinations of (R,T), $Lu_5Rh_4Si_{10}$ is considered to be a prototypical and reference material. It crystallizes in the $Sc_5Co_4Si_{10}$ structure type[2,3] (the tetragonal space group $P4/mbm$) where Sc atoms occupy three different sites. The Lu1 atoms form a chainlike structure along the c axis that is embedded in a network of closely bonded Lu2, Lu3, and Rh atoms. Most probably, the chains of Lu1 atoms carry a quasi-one-dimensional electronic band. The interplay between CDW and superconductivity has been demonstrated by the temperature-pressure phase diagram of $Lu_5Rh_4Si_{10}$.[5] At ambient pressure T_{CDW}=147 K and superconductivity develops below T_c=3.4 K. Increasing the pressure gradually suppresses the CDW transition but T_c jumps from 3.4 K to 4.3 K at 17.9 kbar. There have been also several recent experimental investigations of the nature of the CDW transition in $Lu_5Rh_4Si_{10}$.[17,18] Anomalies at T_{CDW} with thermal hysteresis of about 3 K have been observed in the temperature dependence of the electrical resistivity, magnetic susceptibility, specific heat, thermal conductivity, and thermoelectric power.[17,18] The CDW character is suggested by the fact that these anomalies are in agreement with a decrease of the density of states at the Fermi level. Furthermore, the CDW transition in $Lu_5Rh_4Si_{10}$ is unconventional, as exemplified by the spike-shapes specific heat jump and by a huge entropy change.[17,18] This has led to the speculation that $Lu_5Rh_4Si_{10}$ is a strong interchain coupled CDW system with a first-order phase transition. Here we provide measurements of a key missing property, the electrodynamic response, which enables the CDW in this material to be fully characterized.

Infrared and optical spectroscopic methods are an ideal bulk-sensitive tool to explore the electronic structure and charge dynamics lying behind the CDW transition.[19] To our knowledge, there have been no reports on the optical properties of the ternary silicides. In this paper, we describe the first comprehensive study of the infrared and optical properties of $Lu_5Rh_4Si_{10}$ over a broad spectral range and as a function of temperature. The analysis of the electronic spectral weight and its distribution at low T, as well as the temperature dependence of the scattering rate and the plasma frequency of the itinerant charge carriers extracted from the optical measurements, will be the main goal of this work. The results presented here on $Lu_5Rh_4Si_{10}$ will also provide an interesting counterpoint to other class of low-dimensional conducting systems such as transition-metal trichalocigenides[20] and dichalcogenides.[21–23]

II. EXPERIMENT

The preparation and characterization of polycrystalline $Lu_5Rh_4Si_{10}$ have been described elsewhere.[5] Briefly, samples were grown by arc-melting stoichiometric mixtures of high-purity elements in a Zr-gettered argon atmosphere. The resulting ingots were turned and remelted at least five times to promote homogeneity. Samples were then sealed in quartz ampoules with about 160 Torr of argon and annealed at 1250 °C for one day followed by three days at 1050 °C. The typical grain size of the samples is about 1 μm in diameter. These ceramics were then polished with 0.05 μm grain size

Al_2O_3 powders until an optically reflecting surface was achieved. An x-ray analysis taken with CuK radiation on powder specimens was consistent with the expected $Sc_5Co_4Si_{10}$-type structure, with no other phases present in the diffraction spectrum.

Near-normal optical reflectance measurements were carried out over a wide frequency range using two different spectrometers. A Bruker IFS 66v Fourier transform infrared spectrometer was used in the far-infrared and midinfrared regions (50–6000 cm^{-1}), while the near-infrared to nearultraviolet regions (4000–55000 cm^{-1}) were covered using a Perkin-Elmer Lambda-900 spectrometer. The modulated light beam from the spectrometer was focused onto either the sample or an Au (Al) reference mirror, and the reflected beam was directed onto a detector appropriate for the frequency range studied. The different sources and detectors used in these studies provided substantial spectral overlap, and the reflectance mismatch between adjacent spectral ranges was less than 1%. For low-temperature measurements, the sample was mounted in a continuous flow helium cryostat equipped with a thermometer and heater near the cryostat tip, regulated by a temperature controller.

The optical properties [i.e., the complex conductivity $\sigma(\omega)=\sigma_1(\omega)+i\sigma_2(\omega)$ or dielectric function $\epsilon(\omega)=1+4\pi i\sigma(\omega)/\omega$] were calculated from a Kramers-Kronig analysis of the reflectance data.[24] Because a large frequency region was covered, a Kramers-Kronig analysis should provide reasonably accurate values for the optical constants.[25] To perform these transformations one needs to extrapolate the reflectance at both low and high frequencies. At low frequencies the extension was done by modeling the reflectance using the Drude-Lorentz model and using the fitted results to extend the reflectance below the lowest frequency measured in the experiment. The Hagen-Rubens relation was also used as an extrapolation to low frequencies. Above 60 cm^{-1} the optical conductivity is not sensitive to the choice of low-frequency approximation. The high-frequency extrapolations were done by using a weak power law dependence, $R\sim\omega^{-s}$ with $s\sim 1-2$.

III. RESULTS AND DISCUSSION

Figure 1 shows the measured optical reflectance of $Lu_5Rh_4Si_{10}$ over the entire spectral range at 300 K and 15 K. Note the logarithmic scale. The general shape of room-temperature reflectance displays a metallic character, but the exact position of the plasma minimum is obscured because the free-carrier response overlaps with interband transitions. The inset of Fig. 1 illustrates the optical reflectance from $\approx$50 to 1500 cm^{-1} at several temperatures above and below T_{CDW}. When the sample is cooled from 300 K to 200 K, we do not observe any sharp changes in the optical spectra but rather a continuous evolution-the reflectance increases at most 1%. However, upon crossing $T_{CDW}=147$ K, we see a suppression of far-infrared reflectance and there is an increase in the reflectance in the frequency range between 2000 and 5000 cm^{-1}, indicating that important changes occur in the electronic structures near the Fermi level as a result of the CDW transition. It is worth mentioning that no hysteresis

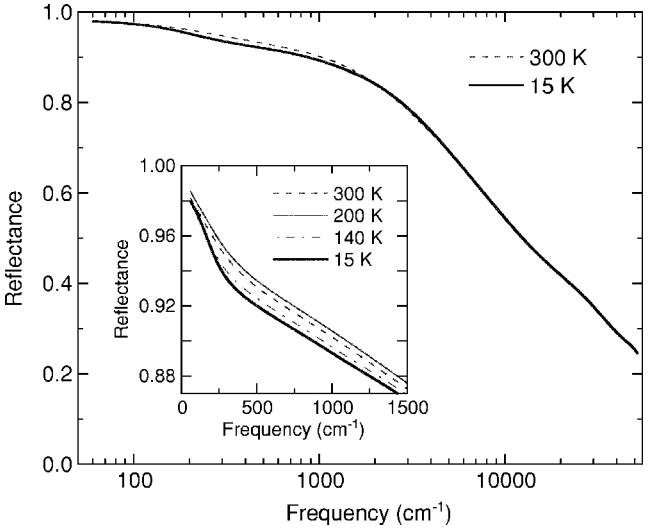

FIG. 1. The reflectance spectra of $Lu_5Rh_4Si_{10}$ at 300 K and 15 K. The data at frequencies above 5000 cm^{-1} do not show any temperature dependence. The inset shows the optical reflectance data of $Lu_5Rh_4Si_{10}$ from 50 to 1500 cm^{-1} and at temperatures above and below T_{CDW}.

effects in the reflectance data were observed within our resolution.

The temperature dependence of the real part of the optical conductivity $\sigma_1(\omega)$, obtained from a Kramers-Kronig analysis of the reflectance, is shown in Fig. 2. There are several important features to these spectra. First, the room-temperature far-infrared conductivity shows canonical metallic behavior, with a line shape in accord with a Drude theory

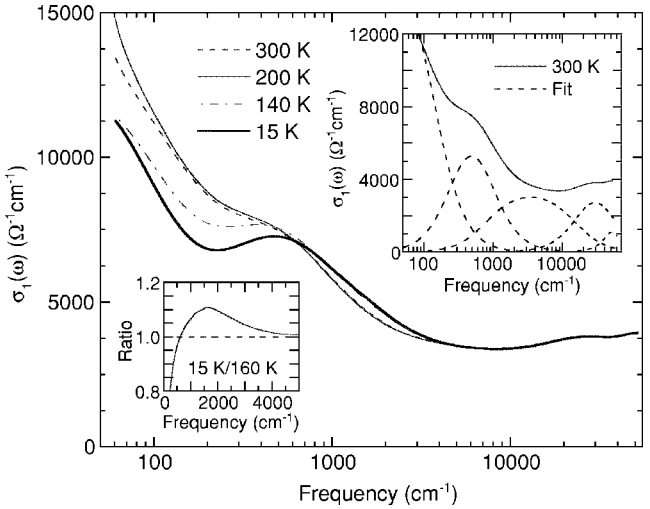

FIG. 2. The real part of the optical conductivity for $Lu_5Rh_4Si_{10}$ at several temperatures, calculated through a Kramers-Kronig analysis of the reflectance spectra presented in Fig. 1. The upper inset shows the 300 K optical conductivity compared to the Drude-Lorentz model calculations. The various terms in the fits are also shown (dashed line): the Drude band and four Lorentz oscillators. The lower inset shows the ratio of $\sigma_1(\omega)$ well below the CDW transition by $\sigma_1(\omega)$ just above the transition. This plot shows the transfer of the spectral weight that accompanies the formation of a CDW state.

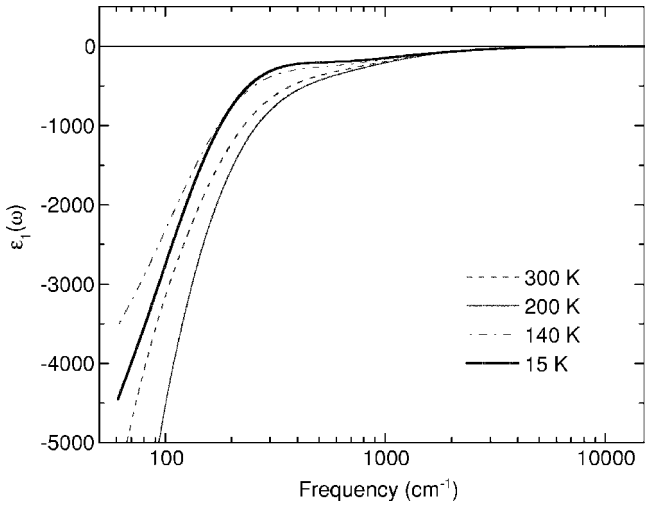

FIG. 3. The real part of the dielectric function $\epsilon_1(\omega)$ (from a Kramers-Kronig transformation) for $Lu_5Rh_4Si_{10}$ at several temperatures.

at least for $\omega < 400$ cm^{-1}. Several interband transitions can be identified at higher frequencies (see below for detailed analysis of interband absorption). Second, with decreasing temperature from 300 K to 200 K, the spectral change is very small-only the low-frequency conductivity increases, in agreement with the metallic dc resistivity behavior. Third, below T_{CDW}, there is a progressive suppression of the optical conductivity in the far-infrared region, which is very reminiscent of the expected scenario for the opening of a gap. In contrast, at high frequencies, $\sigma_1(\omega)$ does not show much temperature variation: all the curves draw together around 5000 cm^{-1}.

Figure 3 displays the real part of the dielectric function at several temperatures above and below T_{CDW}. The rapid decrease in $\epsilon_1(\omega)$ of all temperatures at low frequency is an indication of the metallic behavior (characteristic of free carriers). In a purely Drude system, the zero crossing corresponds to the location of the screened plasma frequency, $\tilde{\omega}_p = \omega_p/\sqrt{\epsilon_\infty}$ where ϵ_∞ is the background dielectric associated with the high-frequency interband transitions, and the plasma frequency ω_p is related to the free carrier density n through $\omega_p = \sqrt{4\pi n e^2/m^*}$. But for $Lu_5Rh_4Si_{10}$, the presence of a number of excitations in the midinfrared will tend to shift the zero crossing to a lower frequency, leading to the uncertainty in the estimation of the value of free carrier density. Thus, we model the reflectance data using the classical Drude-Lorentz dispersion theory[24]:

$$\epsilon(\omega) = -\frac{\omega_{pD}^2}{\omega^2 + i\omega/\tau_D} + \sum_{j=1}^{N} \frac{\omega_{pj}^2}{\omega_j^2 - \omega^2 - i\omega\gamma_j} + \epsilon_\infty, \qquad (1)$$

where ω_{pD} and $1/\tau_D$ are the plasma frequency and the scattering rate of the Drude component; ω_j, γ_j, and ω_{pj} are the frequency, damping, and oscillator strength of the j^{th} Lorentzian contribution; and ϵ_∞ is the high frequency limit of $\epsilon(\omega)$ which includes interband transitions at frequencies above the measured range. The parameters used to fit the measured optical data are listed in Table I. At each temperature the spectrum is well reproduced by considering a Drude-type component due to itinerant charge carriers and four Lorentzian oscillators representing the electronic interband transitions. The fitting results are compared to the 300 K $\sigma_1(\omega)$ in the inset of Fig. 2.

TABLE I. Parameters of a Drude-Lorentz fit for the optical reflectance data. All units are in cm^{-1}.

	T=300 K	T=200 K	T=140 K	T=15 K
ω_{pD}	11820	11870	10710	10200
$1/\tau_D$	143	130	116	107
ω_{p1}	18390	18595	19290	19590
ω_1	486	480	524	528
γ_1	1067	1030	1228	1304
ω_{p2}	53370	54193	54718	56019
ω_2	3442	3440	3180	3180
γ_2	15704	16094	16878	17687
ω_{p3}	96179	95143	94260	93233
ω_3	29120	29120	29120	29120
γ_3	56510	56517	57380	57006
ω_{p4}	48923	52660	50425	51910
ω_4	50660	50660	50660	50660
γ_4	36197	39110	38330	38360
ϵ_∞	3.1	3.1	3.1	3.1

The temperature evolution of ω_{pD} and $1/\tau_D$ is shown in Figs. 4(a) and 4(b). One first observes that the Drude plasma frequency exhibits very little temperature dependence between 300 K and 150 K, whereas the scattering rate monotonically decreases with decreasing temperature. Such behavior is typical of conventional metals.[24] Indeed, the absolute value of the room-temperature Drude plasma frequency implies a carrier density as $n \sim 2.38 \times 10^{21}$ cm^{-3}, under the estimation of $m^*/m_e \sim 1.52$ (m_e is a free-electron mass) from the specific heat measurements.[14] Using the experimental value of $1/\tau_D$, we estimate the carrier mean free path $\ell[=\tau_D \hbar (3\pi^2 n)^{1/3}/m^*] \sim 117$ Å at room temperature, which is much larger than the lattice constant. Second, below T_{CDW}, ω_{pD} is rapidly suppressed and $1/\tau_D$ shows little variation with temperature down to 15 K. Notably, the estimated Drude resistivity [$\rho_{\mathrm{Drude}} = (\omega_{pD}^2 \tau_D/60)^{-1}$, in unit $\mu\Omega$ cm], shown in Fig. 4(c), is in reasonable agreement with the direct dc measurements. This reveals that the dc electrical resistivity anomalies at T_{CDW} are mainly due to changes in the free carrier concentration and not in the lifetime.

Further insight into the charge dynamics can be achieved by exploring changes of the electronic spectral weight in the conductivity,[24]

$$N_{\mathrm{eff}}(\omega)\left(\frac{m_e}{m^*}\right) = \frac{2m_e V_{\mathrm{cell}}}{\pi e^2} \int_0^\omega \sigma_1(\omega')d\omega', \qquad (2)$$

where m_e is taken as the free-electron mass, and V_{cell} is the unit cell volume. $N_{\mathrm{eff}}(\omega)(m_e/m^*)$ is proportional to the number of carriers participating in the optical absorption up to a certain cutoff frequency ω, and has the dimension of fre-

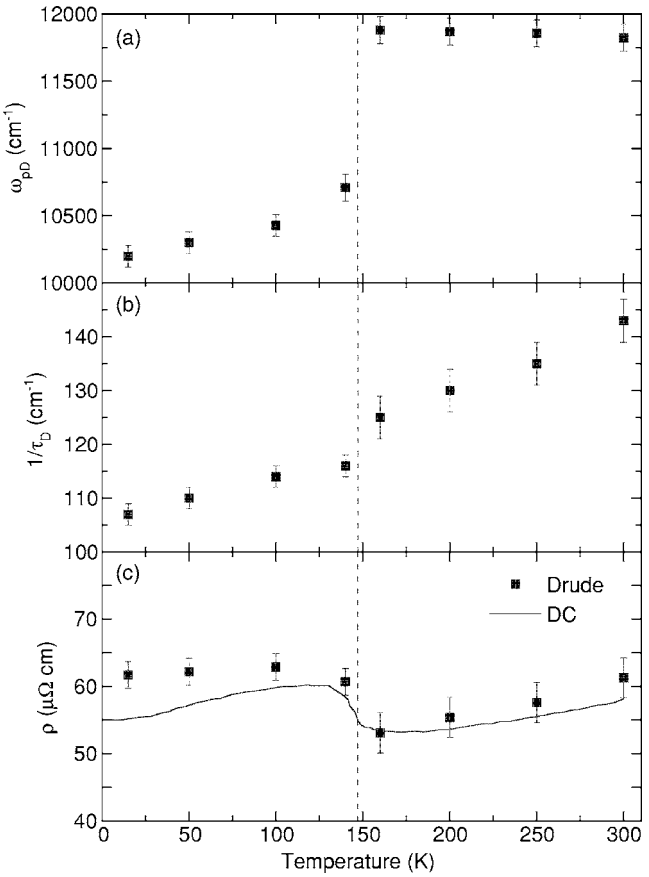

FIG. 4. (a) and (b) The temperature dependence of the Drude plasma frequency ω_{pD} and the Drude scattering rate $1/\tau_D$ from the Drude-Lorentz fit to the optical reflectance spectra of $Lu_5Rh_4Si_{10}$. (c) The Drude resistivity (symbols) from the infrared measurement of $Lu_5Rh_4Si_{10}$ and the dc transport data (solid line) of a similar sample (Ref. 18).

quency squared. Using this procedure we calculated $N_{\text{eff}}(\omega)(m_e/m^*)$ for four temperatures (T=300, 200, 140, and 15 K) and the results are presented in Fig. 5. There are two relevant ranges: the first one above 5000 cm^{-1} up to 10000 cm^{-1} and the second one below 5000 cm^{-1}. In the first range the $N_{\text{eff}}(\omega)(m_e/m^*)$ is temperature independent. In contrast, there is some temperature variation of the spectral weight in the second range. Interestingly, the variation is largest through the CDW transition. The reduction of the spectral weight with decreasing temperatures down to 15 K of the low frequency components of the spectrum, i.e., below 600 cm^{-1}, is fed by a weight gain at higher frequencies extended over an order of magnitude spectral range, i.e., between 600 and 5000 cm^{-1}. We have used finite-frequency sum-rule analysis in Eq. (2) and then calculated the effective number of carriers in the low-frequency region below 5000 cm^{-1} as N_{tot}, the Drude or free-carrier part as N_{Drude} and the midinfrared spectral weight as N_{MIR}. The inset of Fig. 5 shows the fraction changes of the spectral weight among the Drude and midinfrared Lorentz terms as a function of temperature. It is intriguing to note that integration of the conductivity up to ω=5000 cm^{-1}-provides only 10% of the spectral weight we measure when ω is extended up to our

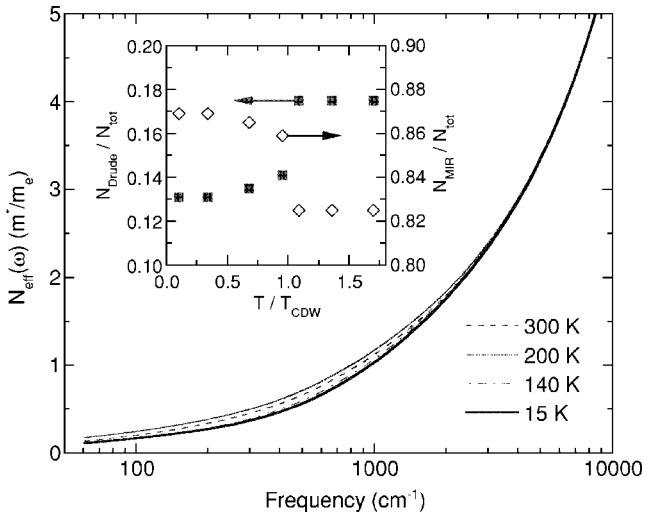

FIG. 5. The temperature dependence of the sum-rule spectra $N_{\text{eff}}(\omega)(m_e/m^*)$ for $Lu_5Rh_4Si_{10}$ at several temperatures. The inset shows the temperature dependence of the fraction changes of the spectral weight among the Drude and midinfrared Lorentz terms.

experiment limit of 55000 cm^{-1}. The Drude term contains about 18% of the total carriers involved in the CDW transition. Furthermore, the strength of the Drude term looses about 4% (i.e., the corresponding plasma frequency decreases) below T_{CDW}. The suppressed Drude weight is transferred to high energies and in particular to the midinfrared absorptions.

We now discuss the implications of the optical data. As mentioned above, in addition to the coherent response of free carriers at ω=0 we observe four absorption bands in the optical conductivity of $Lu_5Rh_4Si_{10}$. All these interband absorption peaks are seen at low temperatures but can be identified even in the 300 K data, which rules out their direct connection to a CDW gap. By lowering the temperature and crossing the CDW transition, a key feature in the data is the evolution of the spectral weight [area under $\sigma_1(\omega)$ curve]—the Drude spectral weight lost by the onset of the CDW state is shifted to the midinfrared frequency range. We propose that the origin of this feature is a pseudogap in the density of states of the quasiparticles that opens in the vicinity of the Fermi level at $T<T_{\text{CDW}}$. This can also be seen in the inset of Fig. 2 where σ_1(15 K)—at which temperature the CDW is almost fully formed-is divided by σ_1(160 K), just above T_{CDW}. The ratio clearly demonstrates the transfer of spectral weight in the CDW state. At frequencies below ~600 cm^{-1}, $\sigma_1(\omega)$ is reduced from the high temperature value while concomitantly increasing at the higher energy region. It is reasonable to take the point that this ratio crosses unity as an approximated upper estimate of the pseudogap (~600 cm^{-1}). Notably, the ratio of $2\Delta/k_BT_{\text{CDW}}$ is ~5.9, which is larger than the mean-field gap parameter value of 3.52. The large difference between the characteristic energy, 2Δ, and the temperature scale for the CDW transition, T_{CDW}, in $Lu_5Rh_4Si_{10}$ is a property exhibited by the strong-coupled CDW system.[12,26,27] Similar evidence has been also inferred from the specific heat measurements.[14,17,18]

Significantly, the development of the CDW pseudogap in $\sigma_1(\omega)$ of $Lu_5Rh_4Si_{10}$ at $T<T_{\text{CDW}}$ suggests that a small frac-

tion of the Fermi surface is gapped by the CDW phase transition. In strict one-dimensional systems, like the well-known blue-bronze $K_{0.3}MoO_3$, the metal-insulator CDW transition manifests itself as a complete transfer of the Drude spectral weight into the CDW gap feature, leading to the formation of a peak at the gap energy. The formation of the peak in the optical conductivity at the gap is also the consequence of the so-called coherence factors.[19] In contrast with the one-dimensional case, however, two-dimensional dichalcogenide materials remain metallic in the presence of CDW since the Fermi surface driven instabilities are generally weaker than in one-dimensional systems. In these two-dimensional conductors, energy gaps can open only at discrete fragments of the Fermi surface, where nesting occurs.[21–23] This leads to a less intensive peak for the CDW gaps in $\sigma_1(\omega)$. In the case of $Lu_5Rh_4Si_{10}$ with a strong interchain coupling, the observed pseudogap-like structure in the charge excitation spectrum is therefore not unexpected due to the three-dimensionality of this material. The depletion of the Drude spectral weight in $\sigma_1(\omega)$ below T_{CDW} is indicative of a progressive gapping of the Fermi surface, which gets partially destroyed at the CDW transition. From the fraction change of the total Drude weight as a function of temperature (the inset of Fig. 5), it is clear that approximately 4% of the Fermi surface in $Lu_5Rh_4Si_{10}$ is destroyed at T_{CDW}, while the rest retains its metallic characters. Other methods for probing the electronic band structure of $Lu_5Rh_4Si_{10}$, such as angle-resolved photoemission spectroscopy and de Haas–van Alphen measurements, would be useful for corroborating our optical data.

Finally, it is worthwhile to ask how CDW fluctuations influence the electrodynamic response of $Lu_5Rh_4Si_{10}$. It is unlikely that the development of the pseudogap we observe in the optical conductivity reflects a precursor fluctuation response associated with the formation of short range CDW segments: while such response should develop above, become maximum near, and diminish below the CDW transition temperature T_{CDW}. Rather, our optical results display the pseudogap feature that evolves at T_{CDW} and grows with decreasing temperature below T_{CDW}. For a quasi-one-dimensional CDW system, one would expect strong fluctuations above T_{CDW}.[28] However, the strong coupling between the chains in $Lu_5Rh_4Si_{10}$ would make the problem more three-dimensional and therefore suppress these fluctuations. Further x-ray scattering experiments currently under way could help to find the conclusive evidence for pretransition fluctuations in $Lu_5Rh_4Si_{10}$.

IV. SUMMARY

In summary, we have performed the first complete optical investigations of $Lu_5Rh_4Si_{10}$. In the high-temperature phase, $T > T_{CDW}$, the optical conductivity consists of a free carrier absorption at zero frequency that narrows rapidly with decreasing temperature, and a much weaker temperature variation of four interband transitions near 486, 3442, 29120, and 50600 cm^{-1}. Below T_{CDW}, the Drude spectral weight is suppressed and transferred to the midinfrared absorption bands, suggesting the opening of a pseudogap $2\Delta \sim 600$ cm^{-1}. The large gap ratio $2\Delta/k_BT_{CDW} \sim 5.9$ associated with this gap is indicative of a strongly coupled CDW transition in $Lu_5Rh_4Si_{10}$. Moreover, a sum-rule evaluation finds that only about 4% of the oscillator strength of the Drude spectral weight is lost due to the CDW formation. Therefore, in addition to the small gapped portions of the Fermi surface involved in the CDW instability, a three-dimensional Fermi surface must also be present, as a result of the strong interchain interactions in $Lu_5Rh_4Si_{10}$. These results highlight exotic metallic properties of $Lu_5Rh_4Si_{10}$ in the broken symmetry ground state.

ACKNOWLEDGMENTS

We thank Y.-K. Kuo for stimulating discussions. This work was supported by the National Science Council of Republic of China under Grant No. NSC 94-2112-M-003-002, 94-2120-M-007-013, 94-2112-M-11-010, and the National Taiwan Normal University under Grant No. ORD93-B.

[1] H. F. Braun and C. U. Segre, Solid State Commun. **35**, 735 (1980).
[2] H. F. Braun, K. Yvon, and R. M. Braun, Acta Crystallogr., Sect. B: Struct. Crystallogr. Cryst. Chem. **36**, 2397 (1980).
[3] H. F. Braun, J. Less-Common Met. **100**, 105 (1984).
[4] R. N. Shelton, L. S. Hausermann-Berg, P. Klavins, H. D. Yang, M. S. Anderson, and C. A. Swenson, Phys. Rev. B **34**, 4590 (1986).
[5] H. D. Yang, P. Klavins, and R. N. Shelton, Phys. Rev. B **43**, 7676 (1991).
[6] H. D. Yang, P. Klavins, and R. N. Shelton, Phys. Rev. B **43**, 7681 (1991).
[7] H. D. Yang, P. Klavins, and R. N. Shelton, Phys. Rev. B **43**, 7688 (1991).
[8] C. A. Swenson, R. N. Shelton, P. Klavins, and H. D. Yang, Phys. Rev. B **43**, 7668 (1991).
[9] K. Ghosh, S. Ramakrishnan, and Girish Chandra, Phys. Rev. B **48**, 4152 (1993).
[10] N. G. Patil and S. Ramakrishnan, Phys. Rev. B **56**, 3360 (1997).
[11] N. G. Patil and S. Ramakrishnan, Phys. Rev. B **59**, 9581 (1999).
[12] B. Becker, N. G. Patil, S. Ramakrishnan, A. A. Menovsky, G. J. Nieuwenhuys, J. A. Mydosh, M. Kohgi, and K. Iwasa, Phys. Rev. B **59**, 7266 (1999).
[13] F. Galli, S. Ramakrishnan, T. Taniguchi, G. J. Nieuwenhuys, J. A. Mydosh, S. Geupel, J. Ludecke, and S. van Smaalen, Phys. Rev. Lett. **85**, 158 (2000).
[14] L. S. Hausermann-Berg and R. N. Shelton, Phys. Rev. B **35**, 6659 (1987).
[15] Sander van Smaalen, Mohammad Shaz, Lukas Palatinus, Peter Daniels, Federica Galli, Gerard J. Nieuwenhuys, and J. A. Mydosh, Phys. Rev. B **69**, 014103 (2004).
[16] Y. K. Kuo, Y. Y. Chen, L. M. Wang, and H. D. Yang, Phys. Rev.

B **69**, 235114 (2004).
[17] C. S. Lue, F. H. Hsu, H. H. Li, H. D. Yang, and Y. K. Kuo, Physica C **364–365**, 243 (2001).
[18] C. S. Lue, Y. K. Kuo, F. H. Hsu, H. H. Li, H. D. Yang, P. S. Fodor, and L. E. Wenger, Phys. Rev. B **66**, 033101 (2002).
[19] G. Grüner, *Density Waves in Solids* (Addison-Wesley, Reading, MA, 1994), and references therein.
[20] A. Perucchi, L. Degiorgi, and R. E. Thorne, Phys. Rev. B **69**, 195114 (2004).
[21] V. Vescoli, L. Degiorgi, H. Berger, and L. Forró, Phys. Rev. Lett. **81**, 453 (1998).
[22] S. V. Dordevic, D. N. Basov, R. C. Dynes, and E. Bucher, Phys. Rev. B **64**, 161103(R) (2001).
[23] S. V. Dordevic, D. N. Basov, R. C. Dynes, B. Ruzicka, V. Vescoli, L. Degiorgi, H. Berger, R. Gaál, L. Forró, and E. Bucher, Eur. Phys. J. B **33**, 15 (2003).
[24] F. Wooten, *Optical Properties of Solids* (Academic, New York, 1972).
[25] We notice that a polycrystalline sample is an inhomogeneous medium whose physical properties vary spatially due to crystal-to-crystal orientation. In our samples, a local response can be justified because the grain size (diameter ~ 0.1 μm after polishing) is much smaller than the wavelength of the light in the range of our interest. Additionally, since $Lu_5Rh_4Si_{10}$ has the nearly three-dimensional structure, its optical constants should be nearly isotropic. The Kramers-Kronig analysis could be applied to our polycrystalline samples without much problem.
[26] Y. K. Kuo, C. S. Lue, F. H. Hsu, H. H. Li, and H. D. Yang, Phys. Rev. B **64**, 125124 (2001).
[27] Y. K. Kuo, F. H. Hsu, H. H. Li, H. F. Huang, C. W. Huang, C. S. Lue, and H. D. Yang, Phys. Rev. B **67**, 195101 (2003).
[28] A. Schwartz, M. Dressel, B. Alavi, A. Blank, S. Dubois, G. Grüner, B. P. Gorshunov, A. A. Volkov, G. V. Kozlov, S. Thieme, L. Degiorgi, and F. Lèvy, Phys. Rev. B **52**, 5643 (1995).